Macromolecules

pubs.acs.org/Macromolecules Article

Topologically Frustrated Dynamical State of Polymers Trapped in Ideal Uniform Tetra-PEG Gels

Di Jia,* Yui Tsuji, Mitsuhiro Shibayama, and Murugappan Muthukumar*

Cite This: https://doi.org/10.1021/acs.macromol.3c01745 Read Online

ACCESS | Metrics & More | Article Recommendations

ABSTRACT: When very long polymers are trapped into multiple entropic traps created by the meshes of host hydrogels, our recent discovery shows that the guest polymer chains are entropically frozen into a nondiffusive topologically frustrated dynamical state (TFDS) at intermediate confinements. Outside the confinement boundaries of the TFDS, the guest molecules diffuse, whereas in the TFDS regime, the center of mass diffusion coefficient is essentially zero due to the macromolecule being localized into long-lived metastable states with extreme free-energy barriers for the escape of the macromolecule. However, the segmental dynamics of the macromolecule is active with hierarchical dynamics. A key assumption to explain this hierarchical segmental dynamics of the macromolecule in the TFDS regime has been that the number of monomers in the various entropic traps is polydisperse. The validity of this assumption is tested in the present paper by experimentally investigating the segmental dynamics using the ideal tetra-PEG hydrogel as the host matrix and sodium poly(styrene sulfonate) as the guest macromolecule. We find that all features of TFDS previously observed using poly(acrylamide-*co*-acrylate) hydrogels with the polydisperse distribution of mesh size are recovered in the present system of uniform mesh size as well. Thus, the present study, with the chemical details different from those of our previous systems, adds credence to the universality of the phenomenon of TFDS. Furthermore, the present finding suggests that the polydispersity in the number of monomers in the various entropic traps must arise from conformational fluctuations emanating from the local exchange dynamics of segments among neighboring meshes.

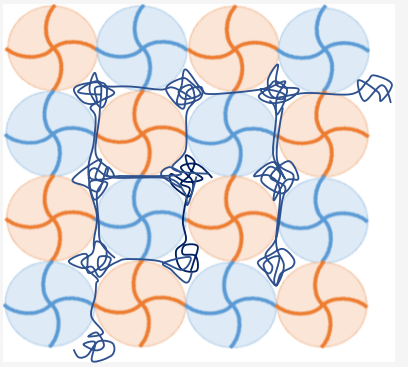

1. INTRODUCTION

Movement of very long polymer chains in restricted environments is ubiquitous in separation science and associated technologies, as well as in crowded biological situations.[1−4] In view of the general premise of this phenomenon, considerable effort has been made toward a fundamental understanding of macromolecular motion in crowded environments.[5−23] While Brownian motion and diffusion of these chains at a finite temperature is the axiom of their motion at ambient conditions, a recent experimental discovery[24,25] based on the dynamics of DNA and synthetic polyelectrolytes, trapped inside a hydrogel at room temperature containing essentially water, has revealed that this axiom is wildly deviated at intermediate confinements.

It is well known that the diffusion of the guest molecules for weaker confinements follows the Zimm−Rouse dynamics,[7,17,20,21] where the condition of weak confinement corresponds to the radius of gyration R_g being much smaller than the mesh size ξ of the gel. As the confinement becomes slightly higher, such that R_g is comparable to ξ, a single entropic barrier between adjacent meshes slows down the diffusion coefficient D of the guest molecules.[8,10,13,22,23] Similarly, when R_g is much larger than ξ and for ξ comparable to monomer length l, the guest molecule undergoes slow diffusion, which is approximately described by the reptation model.[17−20] However, for intermediate confinements ($R_g > \xi > l$), every guest molecule is partitioned into multiple meshes, which function as cooperative entropic traps.[24,25] As a result, for such intermediate confinement conditions, the guest molecules are entropically frozen into an extremely long-lived metastable dynamical state, called the topologically frustrated dynamical state (TFDS). Preliminary theoretical analysis of the role of multiple entropic traps acting on a single large guest macromolecule has shown that the apparent diffusion coefficient of the guest molecule is essentially zero. This unexpected result of $D = 0$ is experimentally validated using the particle tracking method on fluorescently tagged DNA that is trapped inside a hydrogel at intermediate confinements.[26] Furthermore, using this particle tracking method in the presence of an external electric field, the origin of the TFDS is attributed to a large free-energy barrier >100 k_BT (k_BT is the thermal energy),[27,28] which is responsible for plunging the

Received: August 30, 2023
Revised: October 27, 2023
Accepted: November 9, 2023

guest macromolecule into an extremely long-lived nondiffusive metastable state, and hence with $D = 0$.

Even though the diffusion of the guest macromolecule in the TFDS is frozen, previous dynamic light scattering (DLS) experiments[24,25] show that the trapped molecules exhibit hierarchical segmental dynamics, portrayed by

$$g_1(t) \sim e^{-(\frac{t}{\tau})^{\beta}},\ \beta \simeq \frac{1}{3} \tag{1}$$

where $g_1(t)$ is the electric field correlation function measured by DLS, τ is a nonuniversal characteristic relaxation time for the hierarchical dynamics, and the stretched exponent β is about 1/3.

This hierarchical segmental dynamics was conjectured[24,25] to arise from a polydisperse distribution $p(m)$ of the number m of monomers in the meshes due to the inherent polydispersity in the mesh size of the hydrogel. Since hydrodynamics and intermonomer-excluded volume interactions are expected to be screened inside each mesh, the Rouse dynamics is expected inside each mesh that contains m monomers. By relating $g_1(t)$ and the time correlation function of the end-to-end distance of the subchain inside a mesh of size ξ and m monomers, $g_1(t) \sim \exp(-\frac{t}{\tau_R(m)})$, where $\tau_R(m)$ is the Rouse relaxation time proportional to m^2, written as $B_m m^2$ (where B_m is a prefactor). Accounting for the polydispersity in m in different meshes, the net $g_1(t)$ is a convolution of $p(m)$ and the Rouse result for $g_1(t)$, given by

$$g_1(t) \sim \int \mathrm{d}m p(m) e^{-(\frac{t}{B_m m^2})}. \tag{2}$$

Since the confinement free energy F_{conf} associated with squeezing m monomers inside a mesh of size ξ is proportional to m, so that $F_{conf} = A_\xi m$ (where A_ξ is a prefactor),[19] $p(m)$ is given by the Boltzmann weight, $p(m) \sim \exp(-A_\xi m)$. Substituting this in the above equation, we get

$$g_1(t) \sim \int \mathrm{d}m e^{-A_\xi m - t/B_m m^2} \sim e^{-t^{1/3}} \tag{3}$$

in agreement with the experimental findings. It is to be noted that the above argument is only a conjecture, and the origin of the hierarchical dynamics in the TFDS has yet to be fully understood.

The key assumption in the above conjecture is the polydispersity in the number of monomers in the meshes. This polydispersity can arise in three ways: (i) the hydrogel containing the guest molecule is structurally heterogeneous with a polydisperse distribution in mesh size ξ, (ii) thermal fluctuations in the number of monomers inside each mesh due to local dynamical exchange of monomers among neighboring meshes, and (iii) a combination of the above two mechanisms.

In view of this, we address in this paper the role of distribution of the mesh size of the gel on the onset of the topologically frustrated dynamical state. To reach this goal, we have monitored the dynamics of guest poly(styrene sulfonate) molecules trapped inside ideal networks, with narrow mesh size, made from tetra-polyethylene glycol. We report that the topologically frustrated dynamical state still emerges in these ideal gels, suggesting that the origin of the new phenomenon is due to the conformational fluctuations of the various sectors of the guest macromolecule trapped inside the meshes of the host gel.

2. EXPERIMENTAL SECTION

2.1. Materials. Tetra-amine-terminated poly(ethylene glycol) (tetra-PEG-NH_2) with the molecular weight M_w = 40 kDa and tetra-NHS-glutarate-terminated poly(ethylene glycol) (tetra-PEG-NHS) with the molecular weight M_w = 40 kDa were purchased from NOF Co. (Tokyo, Japan). Here, NHS represents *N*-hydroxysuccinimide. Sodium polystyrene sulfonate (NaPSS) with the molecular weights M_w = 2270 kDa and M_w = 68 kDa was purchased from Scientific Polymers. Sodium phosphate, disodium phosphate, and sodium chloride were purchased from Sigma-Aldrich. Hydrophilic polyvinylidene fluoride (PVDF) filters with a pore size of 450 nm were purchased from Millex Company. Deionized water was obtained from a Milli-Q water purification system (Millipore, Bedford, MA, U.S.A.). The resistivity of deionized water used was 18.2 MΩ cm.

2.2. Gel Synthesis and Sample Preparation. Two types of 4-armed poly(ethylene glycol) (PEG) macromonomers with equal arm lengths and with different reactive terminal groups were used to synthesize tetra-PEG gels. Tetra-PEG gels were synthesized by the cross-end coupling of *N*-succinimide (NHS)-terminated tetra-PEG macromonomers and amine-terminated tetra-PEG macromonomers following the previous method.[29−33] Tetra-PEG-NH_2 and tetra-PEG-NHS were dissolved in phosphate buffer to adjust the pH, so that pH = 7.4 for the tetra-PEG-NH_2 solution and pH = 5.8 for the tetra-PEG-NHS solution. The ionic strength of the buffer solution was tuned by adding NaCl. Phosphate buffer with an ionic strength 100 mM (pH 6.8) was used as the solvent. Equimolar quantities of tetra-PEG-NH_2 and tetra-PEG-NHS were mixed with a certain amount of concentrated PSS solution to reach the targeted concentrations for each species. The polymer concentration of the tetra-PEG gel was 60 mg/mL, and the NaPSS concentrations were 0, 5, 20, and 40 mg/mL. Since light scattering measurement is extremely sensitive to dust, the light scattering tubes were first washed with pure water and acetone separately several times. After they were dried in an oven overnight, an aluminum foil was used to wrap up the tubes, and then these tubes were further cleaned by distilled acetone through an acetone fountain setup.[34,35] Then, the pregel solutions were slowly filtered into a light scattering tube through a 450 nm PVDF filter to remove dust. All the sample preparation work was conducted in a superclean bench to avoid any dust. At least 24 h were allowed for the completion of the gelation reaction before the light scattering measurements were performed.

2.3. Static and Dynamic Light Scattering. SLS and DLS measurements were performed on a commercial spectrometer equipped with a multi-τ digital time correlator (ALV-5000/E) with an argon laser light source (output power = 400 mW) of wavelength 514.5 nm. DLS measures the intensity−intensity time correlation function $g_2(t)$ by means of a multichannel digital correlator and is related to the normalized electric field correlation function $g_1(t)$ through the Siegert relation.[36] Measurement was conducted at scattering angles of 30°, 40°, 50°, 60°, and 70°. The relaxation rate Γ at each scattering angle was obtained by averaging the relaxation rates over three different spatial locations within the samples.

2.4. Data Fitting Method. CONTIN method and multiple exponential fitting method were used to analyze the characteristic relaxation rate Γ at each angle.[36−39] Based on $D = \Gamma/q^2$, diffusion coefficient D was calculated. Here, q is the scattering wavevector $q = (4\pi n/\lambda)\sin(\theta/2)$, with the scattering angle θ, wavelength of the incident monochromatic light λ, and refractive index of the medium n. For the correlation functions of NaPSS in the gel matrix, multiple modes were first confirmed by the CONTIN method. In the presence of multiple modes and in order to facilitate comparison to a theory, the normalized electric field correlation function $g_1(t)$ was fitted by a sum of one or two exponential decays and a stretched exponential function.[24,25,40] $g_1(t)$ was fitted using ORIGIN software by the minimization of errors between the fitted prediction and the data. Iterations were performed until the best-fitting curve was obtained within the tolerance limit. The residuals, which are obtained from the difference between the original data and the fitting curve, are

https://doi.org/10.1021/acs.macromol.3c01745
Macromolecules XXXX, XXX, XXX−XXX

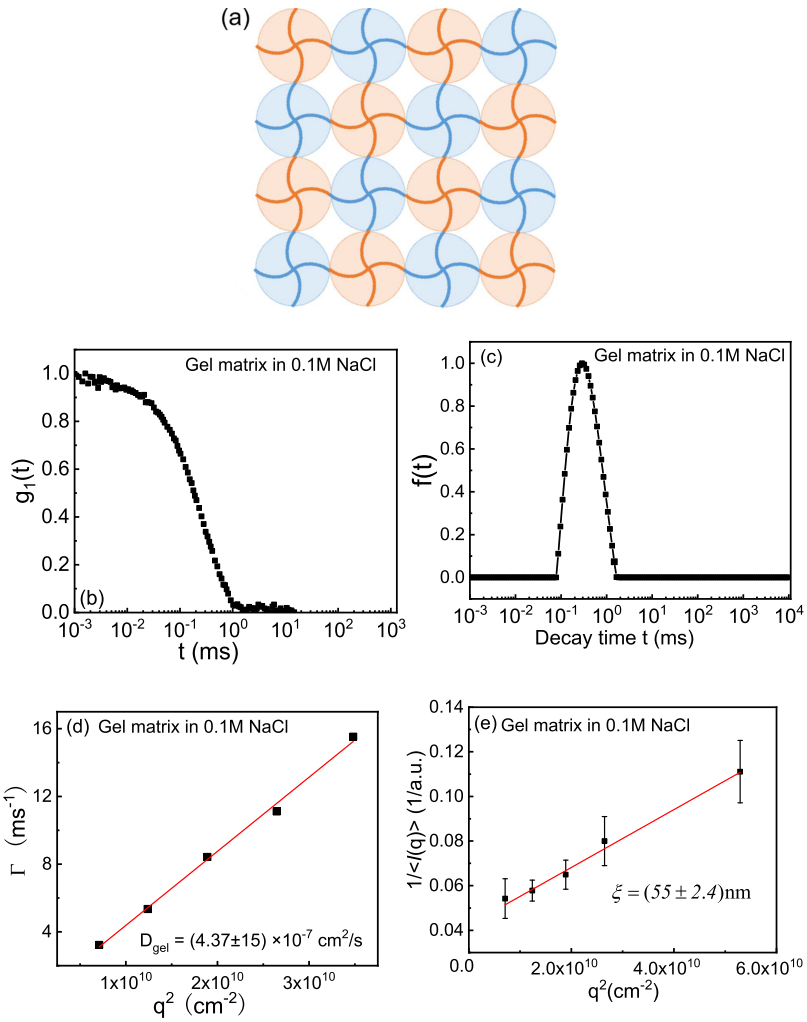

Figure 1. (a) Schematic cartoon of the tetra-PEG gel, with the monodispersed gel mesh size synthesized by cross-linking the end groups of two types of four-arm macromonomers with equal arm lengths. (b−e) Dynamic and static light scattering results for the tetra-PEG gel matrix with 0.1 M NaCl. (b) Normalized field correlation function $g_1(t)$ at a scattering angle of 30° measured by dynamic light scattering. (c) Corresponding relaxation time distribution function obtained from CONTIN fit at a scattering angle of 30°. (d) q^2 dependence of the relaxation rate Γ for the tetra-PEG gel matrix. (e) Ornstein−Zernike plot of the inverse averaged scattering intensity $1/<I(q)>$ versus q^2 measured by static light scattering of the tetra-PEG gel matrix, yielding the large-scale correlation length ξ_c = (55 ± 2.4) nm for concentration fluctuations.

randomly distributed about the mean of zero and do not have systematic fluctuations about their mean.

3. RESULTS AND DISCUSSION

3.1. Characterization of the Gel Matrix. The gel matrix used here was a nominally uncharged tetra-PEG gel with a nearly monodispersed gel mesh size because the tetra-PEG gel was made from two types of four-armed PEG macromonomers with an equal arm length cross-linked through their end groups, as shown in Figure 1a. However, there are still some defects such as rings or dangling ends in the tetra-PEG gel network due to the chemical reaction, and the cartoon in Figure 1a is an ideal gel network model. Static and dynamic light scattering measurements were conducted to characterize the gel matrix. The normalized electric field correlation function $g_1(t)$ and the corresponding relaxation time distribution function obtained from CONTIN fit at a scattering angle of 30 ° as a typical example is shown in Figure 1b,c. Typically, for gels, the correlation function obtained from DLS shows a dominant decay with several other relaxations due to inherent inhomogeneities from the clustering of cross-links and other impurities.[40−43] These inhomogeneities show up as a static electric field, which interferes directly with the scattered electric field from the gel mode. However, here, there is only one mode, indicating that the gel is very homogeneous and clean. Further, the gel mode is diffusion-like, representing the gel elasticity, and the corresponding elastic diffusion coefficient D_{gel} is (4.37 ± 0.15) × 10^{-7} cm^2/s (Figure 1d), which, using the Stokes−Einstein analysis, leads to a mesh size of 5.9 nm. This size is consistent with the estimate of the mesh size from the chemical formula of the mesh. This length cannot be determined using static light scattering, and neutron scattering is required.[33] However, large-scale correlation length for monomer concentration fluctuations can be determined using the static light scattering and the Ornstein−Zernike equation:[36]

$$I(q) = \frac{I(q \to 0)}{1 + q^2\xi_c^2} \tag{4}$$

where $I(q)$ is the static light scattering intensity at the scattering wave vector q, and ξ is the static correlation length of the gel. In the plot of $1/I(q)$ versus q^2, we get ξ_c = (55 ±

https://doi.org/10.1021/acs.macromol.3c01745
Macromolecules XXXX, XXX, XXX−XXX

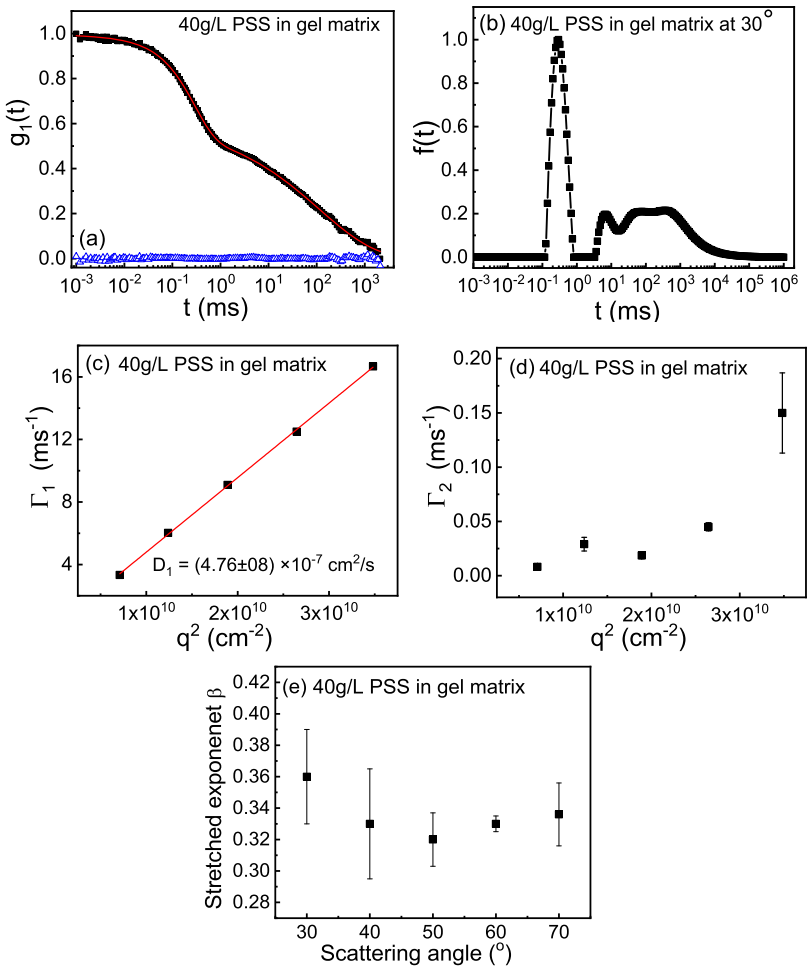

Figure 2. Dynamic light scattering results for 40 g/L NaPSS in the tetra-PEG gel matrix with 0.1 M NaCl. (a) Normalized field-correlation function $g_1(t)$ at a scattering angle of 30°. The blue triangles are the residuals between the original data (black) and the fitting curves (red). (b) Corresponding relaxation time distribution function obtained from the CONTIN fit at the scattering angle of 30°. (c,d) Fitting results of the relaxation rate Γ vs q^2 at all angles for the first and second modes. (e) Stretched exponent β as a plot of different scattering angles for 40 g/L NaPSS in the tetra-PEG gel matrix with 0.1 M NaCl.

2.4) nm from the square root of the slope/intercept ratio, as shown in Figure 1d. This size is much larger than the mesh size of 5.9 nm and indicates roughly the average domain size of the homogeneous ideal tetra-PEG hydrogel, consistent with earlier results.[44]

3.2. Dynamics of Guest Chains in the Tetra-PEG Gel Matrix at High Concentrations. The guest chain used here is NaPSS with M_w = 2270 kDa in 0.1 M NaCl solution. The detailed characterization of NaPSS with M_w = 2270 kDa in 0.1 M NaCl solution is made in our previous studies.[38,43] For NaPSS with M_w = 2270 kDa in 0.1 M NaCl solution, the SLS results show that its radius of gyration is R_g = 96 nm. The DLS results show that there are two diffusive modes representing coupled motion[39,45] among polyions, counterions, and coions and one diffusive mode representing dipole−dipole interaction-induced aggregation mode. The key point here is that when NaPSS chains are in solution, all of the modes are diffusive. However, it is entirely different when the NaPSS guest chains are imbedded inside the gel matrix.

The best fit of the correlation function $g_1(t)$ for 40 g/L NaPSS in the gel matrix can be expressed as (Figure 2a):

$$g_1(t) = a_1 e^{-\Gamma_1 t} + (1 - a_1) e^{-(\Gamma_2 t)^{\beta}} \quad (5)$$

where Γ_1 = 3.45 ms^{-1} and Γ_2 = 0.009 ms^{-1} are the decay rates for the two dynamical modes, a_1 = 0.4 is the weight of the first mode, and the value of the exponent β = 0.36 is a measure of nondiffusive hierarchically dynamical cooperativity of PSS chains in the gel matrix. The nature of the nondiffusive hierarchy of internal chain dynamics is reflected in a broad flat distribution function (instead of a sharp peak) in the CONTIN fitting method, as shown in Figure.2b for the scattering angle of 30°.

Analyzing $g_1(t)$ data at multiple scattering angles reveals that the first mode (exponential decay) is diffusive, which is demonstrated in Figure 2b, where $\Gamma_1 \sim q^2$ with the diffusion coefficient $D_1 = (4.76 \pm 0.08) \times 10^{-7}$ cm^2/s. Since D_1 is very close to the diffusion coefficient of the gel matrix alone (Figure 1d), we assign the first mode as the gel mode, which indicates the gel elasticity ($D_1 = D_{gel}$). Then, the dynamics of all the guest chains come into the second term in eq 2, which is a nondiffusive stretched exponential decay, because Γ_2 is not proportional to q^2 (Figure 2c). Further, the value of β, which indicates the hierarchy of the cooperative local segmental chain dynamics, is independent of scattering angles (Figure 2d), and the averaged value of β over all scattering angles is $\beta = (0.33 \pm 0.04)$. The nondiffusive stretched exponential decay of the guest chain dynamics under confinement is ascribed to the

https://doi.org/10.1021/acs.macromol.3c01745
Macromolecules XXXX, XXX, XXX−XXX

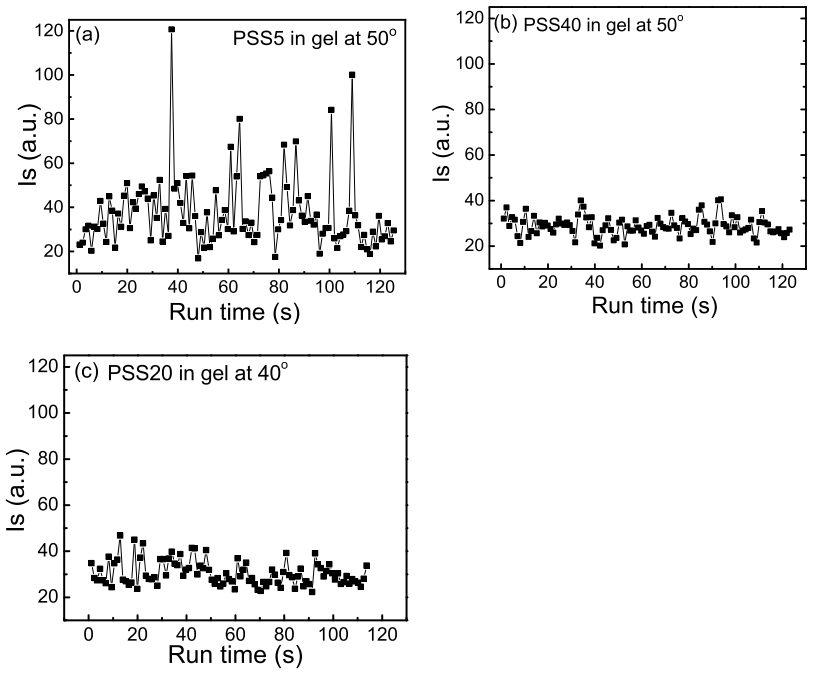

Figure 3. Scattered intensity I_s as a function of running time during the measurements for NaPSS of 5 (a), 40 (b), and 20 g/L (c) in the gel matrix.

nondiffusive topological frustrated dynamics, in which the center of mass of the whole chain cannot diffuse, but within one chain, all the segments can do their local segmental dynamics in a hierarchical way. Further, the β values at all scattering angles are within a very narrow range, which is very different from the traditional temperature-dependent glassy and aging systems, where β is in the full range $(0 < \beta < 1)$.[46] It is also remarkable that all three diffusive modes in solutions are replaced by a nondiffusive stretched exponential mode when the guest chains are inside the gel matrix.

The discovery here is different from our previous studies, since the previous studies are all for the charged system with a negatively charged poly(acrylamide-*co*-sodium acrylate) gel matrix and either negatively or positively charged polyelectrolytes as the guest chains.[24,25] However, in this work, we have used a nominally uncharged tetra-PEG-neutral gel matrix and NaPSS as the guest chains, so that electrostatic interactions between the guest chains and the host gel matrix can be avoided. However, still, we are able to observe the nondiffusive topologically frustrated dynamics in an uncharged gel matrix, demonstrating that such a phenomenon is universal and is ubiquitous for both charged systems and uncharged systems.

As already noted, the mesh size distribution of the tetra-PEG gel matrix is highly monodisperse due to its special synthetic method, while the mesh size distribution of the charged poly(acrylamide-*co*-sodium acrylate) gel is rather polydisperse because it is synthesized by the traditional free-radical polymerization.[47,48] In our earlier work, we had conjectured that the polydispersity of the mesh size in the gel matrix is the origin for the emergence of the nondiffusive topologically frustrated dynamics. However, here, we have observed the same nondiffusive topologically frustrated dynamics in a highly monodisperse uncharged gel matrix, demonstrating that the emergence of the nondiffusive topologically frustrated dynamics is not due to the polydispersity of the mesh size in the gel matrix. Thus, this result leads to the role of thermally induced fluctuations in the number of monomers in the various meshes in eliciting the nondiffusive hierarchical dynamics with $\beta \simeq \frac{1}{3}$.

We note that the tetra-PEG gel is uncharged only approximately. In the pioneering discovery of Reiner et al.,[49] using single-molecule electrophoresis, polyethylene glycol was found to adsorb K^+ ions from the background KCl solution and behave like a polycation. The polycationic behavior of PEG has been reproduced in subsequent studies as well.[50,51] However, the percentage of the net positive charge on the PEG molecule is only 2−5%. Since PSS is considerably more negatively charged, we expect only a minor extent of electrostatic complexation between the tetra-PEG gel and the guest PSS. Assuming that the charge extent of PEG is 4.7% in 10^{-4} M salt solution,[51] we estimate that 13.2 g/L NaPSS can neutralize the effective positive charge on the tetra-PEG matrix. However, at 0.1 M NaCl used in the present study, a higher concentration of NaPSS might be needed to neutralize the tetra-PEG matrix. As addressed in the next section, we estimate this neutralizing concentration of NaPSS as 20 g/L. Therefore, to ensure that the weak electrostatic complexation does not interfere with the deduction of the universal behavior of TFDS, we have taken the concentration of NaPSS as 40 g/L, which is much more than necessary to neutralize 2−5% charge density of the tetra-PEG gel. We address the nature of the complexation between tetra-PEG and PSS at concentrations lower than 40 g/L in the following sections.

3.3. Evidence of Weak Complexation between NaPSS and the Tetra-PEG Gel Matrix. When the concentration of the guest chain in the tetra-PEG gel is low (5 g/L), there are strong fluctuations for the scattered light intensity (Figure 3a), and such strong scattered light intensity fluctuations can easily destroy the scattered light intensity−intensity correlation function $g_2(t)$, so that we cannot obtain any valid correlation function $g_2(t)$.[38,52,53] As shown in Figure 3a, for 5 g/L NaPSS in the gel matrix, the averaged scattered intensity I_s is 30 (a.u.), while the maximum I_s is 120 (a.u.), which is 4 times larger than the average value. Such strong fluctuations of I_s can

https://doi.org/10.1021/acs.macromol.3c01745
Macromolecules XXXX, XXX, XXX−XXX

Table 1. Summary of the Diffusion Coefficient D of NaPSS (M_w = 68 KDa) Solution, Macromonomer Solutions, and the Mixture of NaPSS and Macromonomer Solutions[a]

sample name	diffusion coefficient D
10 g/L NaPSS	$(5.01 \pm 0.13) \times 10^{-7}$ cm^2/s
5 g/L tetra-PEG-NH$_2$	$(3.88 \pm 0.06) \times 10^{-7}$ cm^2/s
5 g/L tetra-PEG-NHS	$(3.87 \pm 0.05) \times 10^{-7}$ cm^2/s
10 g/L NaPSS + 5 g/L tetra-PEG-NH$_2$ mixture	$(2.71 \pm 0.03) \times 10^{-7}$ cm^2/s
10 g/L NaPSS + 5 g/L tetra-PEG-NHS mixture	$(4.05 \pm 0.02) \times 10^{-7}$ cm^2/s

[a]All the samples are with 0.1 M NaCl.

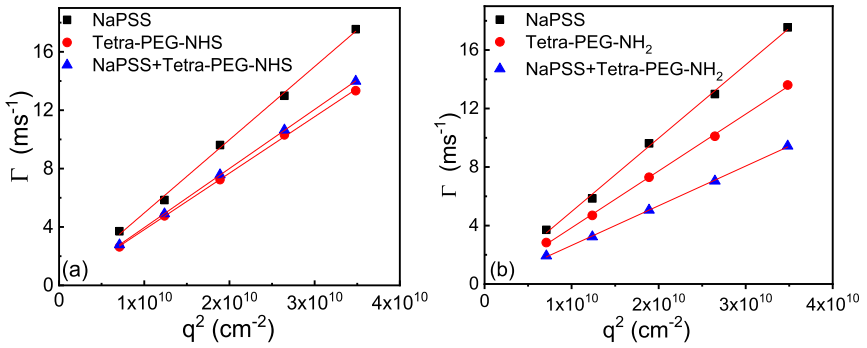

Figure 4. (a) q^2 dependence of the relaxation rate Γ of 10 mg/mL NaPSS (M_w = 68 KDa) solution, 5 mg/mL tetra-PEG-NHS solution, and the mixture of 10 mg/mL NaPSS and 5 mg/mL tetra-PEG-NHS solution. (b) q^2 dependence of the relaxation rate Γ of 10 mg/mL NaPSS (M_w = 68 KDa) solution, 5 mg/mL tetra-PEG-NH$_2$ solution, and the mixture of 10 mg/mL NaPSS and 5 mg/mL tetra-PEG-NH$_2$ solution. All the samples are with 0.1 M NaCl.

immediately destroy the scattered light intensity−intensity correlation function $g_2(t)$, so we cannot get the valid $g_2(t)$ value from the measurement. On the other hand, the fluctuations in the scattered intensity I_s becomes smaller by increasing the concentration of guest molecules NaPSS (such as 40 and 20 g/L), allowing to obtain a valid scattered light intensity−intensity correlation function, as shown in Figure 3b,c.

As noted above, since 5 g/L concentration of NaPSS is lower than the amount necessary to fully neutralize the positively charged tetra-PEG gel, we expect weak complexation between NaPSS chains and the tetra-PEG gel matrix. Such weak complexation can induce strong scattered light intensity fluctuations. When the NaPSS concentration is low, all of NaPSS can weakly complex with the tetra-PEG gel because there are enough complexation sites on the gel. However, when the NaPSS concentration is high, only part of NaPSS can complex and fully saturate the complexation sites on the tetra-PEG gel; then, the extra free NaPSS chains can move around with no complexation, and the I_s signal from the extra free NaPSS chains will dominate over the I_s signal from the weakly complexed NaPSS chains. Therefore, we can successfully observe the topologically frustrated dynamics for the extra uncomplexed guest chains in a fully complexed neutral gel matrix.

In order to further verify such a complexation, we designed an experiment to test the diffusion coefficient D of each species and their mixtures in solutions as follows. We have measured the diffusion coefficients for 5 g/L tetra-PEG-NH$_2$ (M_w = 40 kDa) macromonomer solution, 5 g/L tetra-PEG-NHS macromonomer (M_w = 40 kDa) solution, 10 g/L NaPSS (M_w = 68 kDa) solution, and their mixtures. NaPSS with a low M_w instead of NaPSS with a high M_w = 2270 kDa was chosen for the complexation study in solution because the DLS result for NaPSS with M_w = 2270 kDa alone in 0.1 M NaCl solution is already complicated,[39] so it is not suitable for the complexation study between NaPSS and the tetra-PEG macromonomer. Therefore, NaPSS with a low M_w, which has only one dynamical mode in DLS, was chosen for the complexation study. Further, such complexation between NaPSS and the tetra-PEG macromonomer should be independent of the M_w of NaPSS.

The concentrations are chosen so that each species is below their overlap concentration C*, so that the viscosity of the dilute solutions does not change much. All the samples are prepared with 0.1 M NaCl. The results are shown in Table 1 and Figure 4. For 10 g/L NaPSS (M_w = 68 kDa) in 0.1 M NaCl solution, there is only one mode with the diffusion coefficient $D = (5.01 \pm 0.13) \times 10^{-7}$ cm^2/s. For two types of macromonomers, $D = (3.88 \pm 0.06) \times 10^{-7}$ cm^2/s for 5 g/L tTetra-PEG-NH$_2$ in 0.1 M NaCl solution and $D = (3.87 \pm 0.05) \times 10^{-7}$ cm^2/s for 5 g/L tTetra-PEG-NHS in 0.1 M NaCl solution. When 10 g/L NaPSS is mixed with 5 g/L tTetra-PEG-NHS solution, $D = (4.05 \pm 0.02) \times 10^{-7}$ cm^2/s, which is close to D of tetra-PEG-NHS alone and much lower than D of NaPSS alone. Further, when 10 g/L NaPSS is mixed with 5 g/L tetra-PEG-NH$_2$ solution, $D = (2.71 \pm 0.03) \times 10^{-7}$ cm^2/s, which is lower than D of both NaPSS alone and tetra-PEG-NH$_2$ alone. These data clearly indicate that NaPSS (10 g/L) is able to complex with tetra-PEG in 0.1 M NaCl and that the complexation with tetra-PEG-NH$_2$ is significant.

3.4. Dynamics of the Guest Chains in the Neutral Gel Matrix at Intermediate Concentrations. As mentioned above, the NaPSS concentration required to fully neutralize the tetra-PEG gel matrix is around 20 g/L. This estimate is based on the emergence of a valid correlation function $g_2(t)$ at 20 g/L NaPSS concentration (see also Figure 3c). The correlation functions at the scattering angles 30° and 50° are shown in Figure 5a,b, and the best fit of $g_1(t)$ can be accomplished by the sum of one exponential decay, one stretched exponential

https://doi.org/10.1021/acs.macromol.3c01745
Macromolecules XXXX, XXX, XXX−XXX

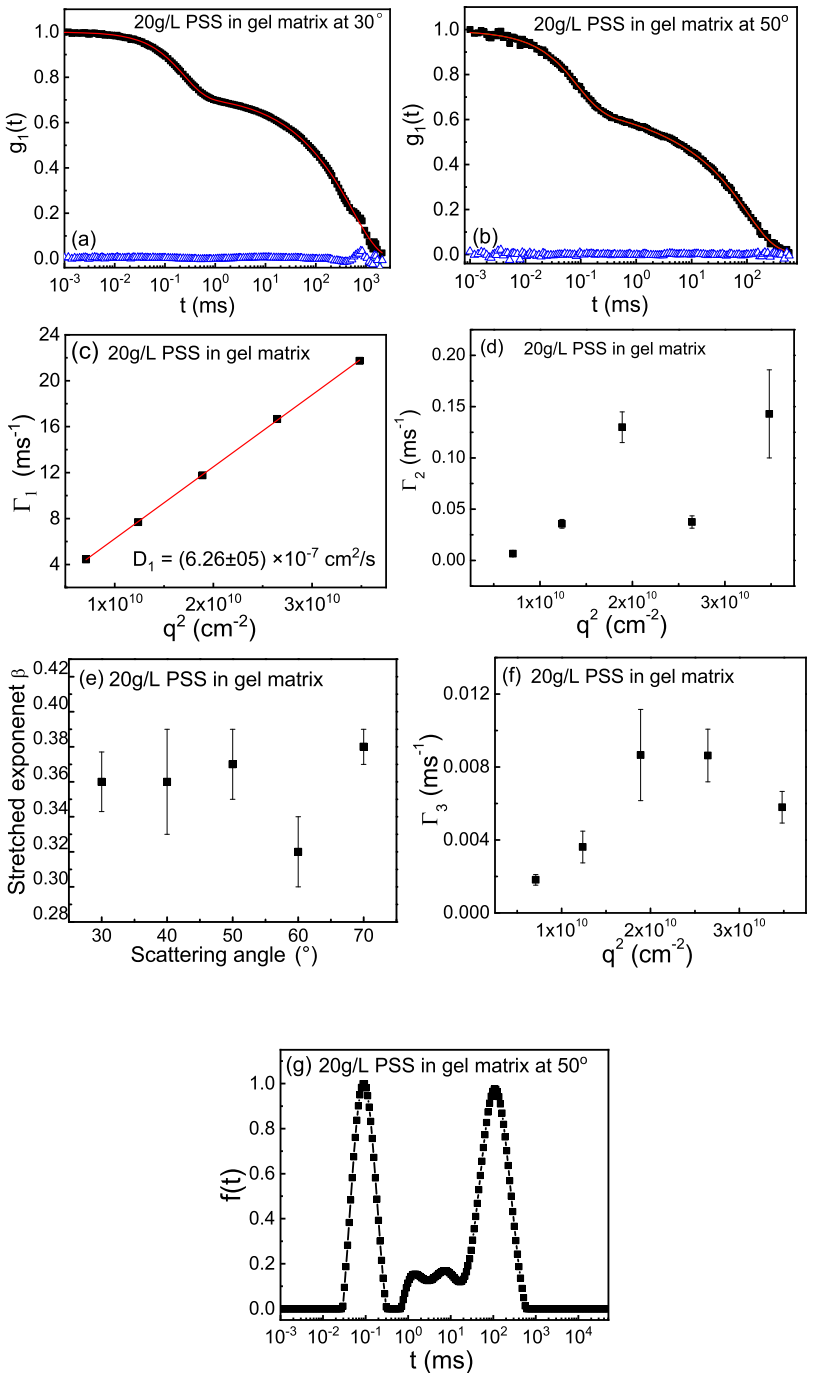

Figure 5. Dynamics of NaPSS chains at 20 g/L in the tetra-PEG gel matrix with 0.1 M NaCl. (a,b) Normalized field-correlation function $g_1(t)$ at scattering angles of 30° and 50°, respectively. The blue triangles are the residuals between the original data (black) and the fitting curves (red). (c,d) Fitting results of the relaxation rate Γ_1 and Γ_2 vs q^2 at all angles for the first and second modes, respectively. (e) Stretched exponent β as a plot of different scattering angles for 20 g/L NaPSS in the tetra-PEG gel matrix with 0.1 M NaCl. (f) Fitting results of the relaxation rate Γ_3 vs q^2 at all angles for the third mode. (g) Corresponding relaxation time distribution function obtained from the CONTIN fit at the scattering angle of 50°.

decay, and another exponential decay with a much larger decay time (ultraslow mode), expressed as below:

$$g_1(t) = a_1 e^{-\Gamma_1 t} + a_2 e^{-(\Gamma_2 t)^{\beta}} + (1 - a_1 - a_2) e^{-\Gamma_3 t} \quad (6)$$

The analysis of DLS data on the decay rates at different scattering angles shows that Γ_1 is diffusive with the corresponding diffusion coefficient $D_1 = (6.26 \pm 0.05) \times 10^{-7}$ cm^2/s, which is the gel mode (Figure 5c). The presence of NaPSS introduces an additional elastically coupled domain that may lead to a more rapid relaxation of the gel mode fluctuations; thus, D_{gel} is higher than that of the gel matrix without NaPSS. The second mode is a nondiffusive stretched exponential decay since Γ_2 is not proportional to q^2 (Figure 5d). Further, the value of β over all the scattering angles is $\beta = (0.36 \pm 0.03)$ (Figure 5e). The third mode is also a nondiffusive single-exponential decay because Γ_3 is not proportional to q^2; so, it is a nondiffusive mode (Figure 5f). Because 20 g/L NaPSS is around the threshold concentration to fully complex and neutralize the tetra-PEG gel matrix, the

https://doi.org/10.1021/acs.macromol.3c01745
Macromolecules XXXX, XXX, XXX−XXX

third nondiffusive mode with a much slower decay rate Γ_3 (ultraslow mode) may come from the fluctuations or the heterogeneity due to the weak complexation between NaPSS and the tetra-PEG gel matrix (Figure 5f). Since the value of Γ_3 is much smaller than that of Γ_2 and Γ_1, we can decouple the third ultraslow mode from the second stretched exponential mode, which indicates the hierarchical segmental dynamics for the guest chains, although both the second and third modes are nondiffusive (since both Γ_2 and Γ_3 are not proportional to q^2). In order to demonstrate the coexistence of the three modes, the CONTIN fitting method was used. The corresponding relaxation time distribution function obtained from the CONTIN fitting method at the scattering angle of 50° is shown in Figure 5g. For such a complex system, although three modes can be roughly confirmed by the CONTIN fitting method, the second mode expressed by a stretched exponential decay appears only as a broad flat distribution as in the case of Figure 2b.

4. CONCLUSIONS

As in our previous study using poly(acrylamide-*co*-acrylate) hydrogels as the host gel, where the mesh size of the gel is not uniform, we find the same phenomenon of the nondiffusive hierarchical dynamics with the ideal tetra-PEG hydrogels as the host gel, where the mesh size is uniform. This finding demonstrates that the mesh size distribution of the matrix is not critical to elicit the topologically frustrated dynamical state. Furthermore, since we find the same value of β around 1/3 for both systems, we conclude that this new dynamical state is universal. Based on this observation, we conclude that the required polydispersity in the number of monomers inside gel meshes, for the emergence of hierarchical dynamics, must arise from thermal fluctuations.

In addition, our experiments show that nominally neutral tetra-PEG acts like a very weak polycation under the electrolyte concentration studied here. This is evident from the weak complexation between NaPSS chains and the tetra-PEG gel matrix, which leads to strong scattered light intensity fluctuations. Our conclusions on the features of TFDS are reached by ensuring that the concentration of the guest macromolecules is very much higher than that necessary to neutralize the weak positive charges on the tetra-PEG matrix.

Lastly, although the tetra-PEG gel used here can be regarded as an ideal physical model with a uniform gel mesh size and much fewer defects compared to other types of gels synthesized by using free-radical polymerization, it is not an absolute ideally perfect gel matrix. Rose et al. have utilized particles with different sizes to probe the defects with different length scales in the tetra-PEG gels.[54] Recently, there are even more "perfect" and defect-free gels developed by using other advanced synthetic methods.[31,32] Exploration of such gels and induction of enhanced conformational fluctuations of the guest macromolecule by varying the mesh size in ideal gels are relegated to future works.

AUTHOR INFORMATION

Corresponding Authors

Di Jia − *Department of Polymer Science and Engineering, University of Massachusetts Amherst, Amherst, Massachusetts 01003, United States; Beijing National Laboratory for Molecular Sciences, Laboratory of Polymer Physics and Chemistry, Institute of Chemistry, Chinese Academy of Sciences, Beijing 100190, China; University of Chinese Academy of Sciences, Beijing 100049, China;* Email: jiadi11@iccas.ac.cn

Murugappan Muthukumar − *Department of Polymer Science and Engineering, University of Massachusetts Amherst, Amherst, Massachusetts 01003, United States;* orcid.org/0000-0001-7872-4883; Email: muthu@polysci.umass.edu

Authors

Yui Tsuji − *Department of Polymer Science and Engineering, University of Massachusetts Amherst, Amherst, Massachusetts 01003, United States; Institute for Solid State Physics, The University of Tokyo, Kashiwa 277-8581, Japan*

Mitsuhiro Shibayama − *Institute for Solid State Physics, The University of Tokyo, Kashiwa 277-8581, Japan; Neutron Science and Technology Center, Comprehensive Research Organization for Science and Society, Tokai, Ibaraki 319-1106, Japan;* orcid.org/0000-0002-8683-5070

Complete contact information is available at: https://pubs.acs.org/10.1021/acs.macromol.3c01745

Notes

The authors declare no competing financial interest.

ACKNOWLEDGMENTS

M.M. acknowledges financial support from the National Science Foundation (DMR-2309539) and AFOSR (Grant No. FA9550-20-1-0142). D.J. acknowledges financial support from National Natural Science Foundation of China (22273114) and International Partnership Program of the Chinese Academy of Sciences (Grant No. 027GJHZ2022061FN).

REFERENCES

(1) Zhang, Y. S.; Khademhosseini, A. Advances in engineering hydrogels. *Science* **2017**, *356*, No. eaaf3627.

(2) Li, J.; Mooney, D. J. Designing hydrogels for controlled drug delivery. *Nat. Rev. Mater.* **2016**, *1*, 16071.

(3) Alberts, B.; Information, N. C. F. B. *Mol. Biol. Cell*; Garland, 1994.

(4) Kim, J. J.; Park, K. Smart hydrogels for bioseparation. *Bioseparation* **1998**, *7*, 177−184.

(5) Nykypanchuk, D.; Strey, H. H.; Hoagland, D. A. Brownian Motion of DNA Confined Within a Two-Dimensional Array. *Science* **2002**, *297*, 987−990.

(6) Pajevic, S.; Bansil, R.; Konak, C. Diffusion of linear polymer chains in methyl methacrylate gels. *Macromolecules* **1993**, *26*, 305−312.

(7) Zimm, B. H. Dynamics of Polymer Molecules in Dilute Solution: Viscoelasticity, Flow Birefringence and Dielectric Loss. *J. Chem. Phys.* **1956**, *24*, 269−278.

(8) Muthukumar, M.; Baumgaertner, A. Effects of entropic barriers on polymer dynamics. *Macromolecules* **1989**, *22*, 1937−1941.

(9) Smisek, D. L.; Hoagland, D. A. Electrophoresis of Flexible Macromolecules: Evidence for a New Mode of Transport in Gels. *Science* **1990**, *248*, 1221−1223.

(10) Muthukumar, M. Entropic barrier model for polymer diffusion in concentrated polymer solutions and random media. *J. Non-Cryst. Solids* **1991**, *131*, 654−666.

(11) Rousseau, J.; Drouin, G.; Slater, G. W. Entropic Trapping of DNA During Gel Electrophoresis: Effect of Field Intensity and Gel Concentration. *Phys. Rev. Lett.* **1997**, *79*, 1945−1948.

(12) Liu, L.; Li, P.; Asher, S. A. Entropic trapping of macromolecules by mesoscopic periodic voids in a polymer hydrogel. *Nature* **1999**, *397*, 141−144.

(13) Hoagland, D. A.; Muthukumar, M. Evidence for entropic barrier transport of linear, star, and ring macromolecules in electrophoresis gels. *Macromolecules* **1992**, *25*, 6696−6698.
(14) Zimm, B. H. "Lakes−straits" model of field-inversion gel electrophoresis of DNA. *J. Chem. Phys.* **1991**, *94*, 2187−2206.
(15) Parrish, E.; Caporizzo, M. A.; Composto, R. J. Network confinement and heterogeneity slows nanoparticle diffusion in polymer gels. *J. Chem. Phys.* **2017**, *146*, 203318.
(16) Ogston, A. G.; Preston, B. N.; Wells, J. D.; Snowden, J. M. On the transport of compact particles through solutions of chain-polymers. *Proc. R. Soc. Lond. A.* **1973**, *333*, 297−316.
(17) de Gennes, P. G. Reptation of a Polymer Chain in the Presence of Fixed Obstacles. *J. Chem. Phys.* **1971**, *55*, 572−579.
(18) Slater, G. W.; Yan Wu, S. Reptation, Entropic Trapping, Percolation, and Rouse Dynamics of Polymers in "Random" Environments. *Phys. Rev. Lett.* **1995**, *75*, 164−167.
(19) de Gennes, P. G. *Scaling Concepts in Polymer Physics*; Cornell University Press, 1979.
(20) Doi, M.; Edwards, S. F.; Edwards, S. F. *The Theory of Polymer Dynamics*; Clarendon Press, 1986.
(21) Rouse, P. E., Jr. A Theory of the Linear Viscoelastic Properties of Dilute Solutions of Coiling Polymers. *J. Chem. Phys.* **1953**, *21*, 1272−1280.
(22) Lodge, T. P.; Rotstein, N. A. Tracer diffusion of linear and star polymers in entangled solutions and gels. *J. Non-Cryst. Solids* **1991**, *131*−*133*, 671−675.
(23) Rotstein, N. A.; Lodge, T. P. Tracer diffusion of linear polystyrenes in poly(vinyl methyl ether) gels. *Macromolecules* **1992**, *25*, 1316−1325.
(24) Jia, D.; Muthukumar, M. Topologically frustrated dynamics of crowded charged macromolecules in charged hydrogels. *Nat. Commun.* **2018**, *9*, 2248.
(25) Jia, D.; Muthukumar, M. Electrostatically Driven Topological Freezing of Polymer Diffusion at Intermediate Confinements. *Phys. Rev. Lett.* **2021**, *126*, No. 057802.
(26) Chen, K.; Muthukumar, M. Entropic barrier of topologically immobilized DNA in hydrogels. *Proc. Natl. Acad. Sci. U.S.A.* **2021**, *118*, No. e2106380118.
(27) Chen, K.; Li, S.-F.; Muthukumar, M. Boundaries of the Topologically Frustrated Dynamical State in Polymer Dynamics. *ACS Macro Lett.* **2022**, *11*, 699−705.
(28) Chen, K.; Muthukumar, M. Substantial Slowing of Electrophoretic Translocation of DNA through a Nanopore Using Coherent Multiple Entropic Traps. *ACS Nano* **2023**, *17*, 9197−9208.
(29) Sakai, T.; Matsunaga, T.; Yamamoto, Y.; Ito, C.; Yoshida, R.; Suzuki, S.; Sasaki, N.; Shibayama, M.; Chung, U.-I. Design and Fabrication of a High-Strength Hydrogel with Ideally Homogeneous Network Structure from Tetrahedron-like Macromonomers. *Macromolecules* **2008**, *41*, 5379−5384.
(30) Kurakazu, M.; Katashima, T.; Chijiishi, M.; Nishi, K.; Akagi, Y.; Matsunaga, T.; Shibayama, M.; Chung, U.-I.; Sakai, T. Evaluation of Gelation Kinetics of Tetra-PEG Gel. *Macromolecules* **2010**, *43*, 3935−3940.
(31) Li, X.; Nakagawa, S.; Tsuji, Y.; Watanabe, N.; Shibayama, M. Polymer gel with a flexible and highly ordered three-dimensional network synthesized via bond percolation. *Sci. Adv.* **2019**, *5*, No. eaax8647.
(32) Shibayama, M.; Li, X.; Sakai, T. Precision polymer network science with tetra-PEG gels—a decade history and future. *Colloid Polym. Sci.* **2019**, *297*, 1−12.
(33) Matsunaga, T.; Sakai, T.; Akagi, Y.; Chung, U.-I.; Shibayama, M. SANS and SLS Studies on Tetra-Arm PEG Gels in As-Prepared and Swollen States. *Macromolecules* **2009**, *42*, 6245−6252.
(34) Jia, D.; Muthukumar, M.; Cheng, H.; Han, C. C.; Hammouda, B. Concentration Fluctuations near Lower Critical Solution Temperature in Ternary Aqueous Solutions. *Macromolecules* **2017**, *50*, 7291−7298.
(35) Jia, D.; Zuo, T.; Rogers, S.; Cheng, H.; Hammouda, B.; Han, C. C. Re-entrance of Poly(N,N-diethylacrylamide) in D2O/d-Ethanol Mixture at 27 °C. *Macromolecules* **2016**, *49*, 5152−5159.
(36) Han, C. C.; Akcasu, A. Z. *Scattering and Dynamics of Polymers: Seeking Order in Disordered Systems*; Wiley, 2011.
(37) Provencher, S. W. CONTIN: A general purpose constrained regularization program for inverting noisy linear algebraic and integral equations. *Comput. Phys. Commun.* **1982**, *27*, 229−242.
(38) Berne, B. J.; Pecora, R. *Dynamic Light Scattering: With Applications to Chemistry, Biology, and Physics*; Dover: New York, 1976.
(39) Jia, D.; Muthukumar, M. Effect of Salt on the Ordinary−Extraordinary Transition in Solutions of Charged Macromolecules. *J. Am. Chem. Soc.* **2019**, *141*, 5886−5896.
(40) Jia, D.; Muthukumar, M. Interplay between Microscopic and Macroscopic Properties of Charged Hydrogels. *Macromolecules* **2020**, *53*, 90−101.
(41) Morozova, S.; Hamilton, P.; Ravi, N.; Muthukumar, M. Development of a Vitreous Substitute: Incorporating Charges and Fibrous Structures in Synthetic Hydrogel Materials. *Macromolecules* **2016**, *49*, 4619−4626.
(42) Morozova, S.; Muthukumar, M. Elasticity at Swelling Equilibrium of Ultrasoft Polyelectrolyte Gels: Comparisons of Theory and Experiments. *Macromolecules* **2017**, *50*, 2456−2466.
(43) Jia, D.; Muthukumar, M. Theory of Charged Gels: Swelling, Elasticity, and Dynamics. *Gels* **2021**, *7*, 49.
(44) Tsuji, Y.; Nakagawa, S.; Gupit, C. I.; Ohira, M.; Shibayama, M.; Li, X. Selective Doping of Positive and Negative Spatial Defects into Polymer Gels by Tuning the Pregel Packing Conditions of Star Polymers. *Macromolecules* **2020**, *53*, 7537−7545.
(45) Muthukumar, M. Collective dynamics of semidilute polyelectrolyte solutions with salt. *J. Polym. Sci. B. Polym. Phys.* **2019**, *57*, 1263−1269.
(46) Roth, C. B. *Polymer Glasses*; CRC Press, 2016.
(47) Tanaka, T.; Nishio, I.; Sun, S.-T.; Ueno-Nishio, S. Collapse of Gels in an Electric Field. *Science* **1982**, *218*, 467−469.
(48) McCoy, J. L.; Muthukumar, M. Dynamic light scattering studies of ionic and nonionic polymer gels with continuous and discontinuous volume transitions. *J. Polym. Sci. B. Polym. Phys.* **2010**, *48*, 2193−2206.
(49) Reiner, J. E.; Kasianowicz, J. J.; Nablo, B. J.; Robertson, J. W. F. Theory for polymer analysis using nanopore-based single-molecule mass spectrometry. *Proc. Natl. Acad. Sci. U.S.A.* **2010**, *107*, 12080−12085.
(50) Cao, N.; Zhao, Y.; Chen, H.; Huang, J.; Yu, M.; Bao, Y.; Wang, D.; Cui, S. Poly(ethylene glycol) Becomes a Supra-Polyelectrolyte by Capturing Hydronium Ions in Water. *Macromolecules* **2022**, *55*, 4656−4664.
(51) Zhou, C.; Ji, C.; Nie, Y.; Yang, J.; Zhao, J. Poly(ethylene oxide) Is Positively Charged in Aqueous Solutions. *Gels* **2022**, *8*, 213.
(52) Schmitz, K. S. *Introduction to Dynamic Light Scattering by Macromolecules*; Academic Press: San Diego, 1990.
(53) Chu, B. *Laser Light Scattering: Basic Principles and Practice*; Academic Press: New York, 1991.
(54) Rose, K. A.; Marino, E.; O'Bryan, C. S.; Murray, C. B.; Lee, D.; Composto, R. J. Nanoparticle dynamics in hydrogel networks with controlled defects. *Soft Matter* **2022**, *18*, 9045.

https://doi.org/10.1021/acs.macromol.3c01745
Macromolecules XXXX, XXX, XXX−XXX